Online ISSN 1848-3380, Print ISSN 0005-1144
ATKAFF 55(1), 99–111(2014)

Majid Mehrasa, Masoud Ahmadigorji, Nima Amjady

A New Dual Lagrangian Model and Input/Output Feedback Linearization Control of 3-Phase/Level NPC Voltage-Source Rectifier

DOI 10.7305/automatika.2014.01.230
UDK 681.516.013.017-55:621.314.6.025.3
IFAC 2.4.0.1; 4.6.2.1

Original scientific paper

An input/output feedback linearization control strategy is developed for control of three-level three-phase neutral-point-clamped rectifier using its dual Lagrangian modeling. The load current of the rectifier can be given in two forms: (i) the load current involving the current of capacitor C_1 (ii) the load current involving the current of capacitor C_2. Applying the obtained load current to the Euler-Lagrange parameters of the rectifier, two nonlinear models of the system are derived. The models are based on the superposition law of the load current and the Euler-Lagrange description of the rectifier. Also, the two power-balance equations between the input and output sides are obtained by considering the effects of two load currents separately. Then, the two nonlinear models and power-balance equations are linearized using input–output feedback linearization, and the state feedback law controlled inputs are completed by pole placement. With the definition of outputs of the feedback linearization law, the zero dynamics of the system are avoided and a fast output voltages control scheme is designed. Finally, some integrators are added to robust control against parasitic elements. The proposed nonlinear controller is compared to the PI controller and the MATLAB/SIMULINK results verify the proposed control strategy.

Key words: Euler–Lagrange (EL) model, 3 level/phase NPC rectifier, Input/output feedback linearization, Power-balance equations, State feedback law controlled inputs

Novi dualni Langrangeov model i upravljanje trofaznim trorazinskim NPC naponskim ispravljačem zasnovano na ulazno/izlaznoj linearizaciji u povratnoj vezi. Upravljačka strategija zasnovana na ulazno/izlaznoj linearizaciji u povratnoj vezi razvijena je za upravljanje trofaznog trorazinskog ispravljača u spoju sa zajedničkom srednjom točkom korištenjem njegova dualnog Lagrangian modeliranja. Struja trošila ispravljača može se prikazati u dvije forme: (i) struja trošila koja uključuje struje obaju kapaciteta C_1 (ii) struja trošila koja uključuje samo struju kapaciteta C_2. Primjenom dobivene struje trošila na Euler-Lagrangeove parametre ispravljača izvedena su dva nelinearna modela sustava. Modeli su zasnovani na zakonu superpozicije struje trošila i Euler-Lagrangeova opisa ispravljača. Dobivena su dva zakona o ravnoteži snaga između ulazne i izlazne strane uzimajući u obzir učinke dvaju struja trošila zasebno. Dva su nelinearna modela i zakoni o ravnoteži snaga zatim linearizirani pomoću ulazno/izlazne linearizacije u povratnoj vezi i ulazi su upravljani s povratnom vezom po varijablama stanja uz metodu odabira polova sustava. Definiranjem izlaza upravljačkog zakona zasnovanog na linearizaciji po povratnoj vezi, zaobišla se dinamika nula u sustavu te je dizajnirana shema s brzim upravljanjem izlaznim naponima. Naposlijetku, integratori su dodani za postizanje robusnosti na parazitske elemente. Predloženi nelinearni regulator uspoređen je s PI regulatorom, a rezultati su provjereni u MATLAB/SIMULINK okruženju.

Ključne riječi: Euler–Lagrangeov (EL) model, trofazni trorazinski NPC ispravljač, linearizacija pomoću ulazno/izlazne povratne veze, jednadžbe ravnoteže snage, upravljanje po varijablama stanja

1 INTRODUCTION

Multilevel converters permit reaching voltage levels up to medium-voltage drives in the industrial environment. The converters are significantly used for medium-voltage and high-power applications [1-4]. Among these topologies, multilevel neutral-point-clamped (NPC) converters are the most widely used because of their advantages such as series connection of power switches and bi-directional power transfer capability.

However, one of the considerable problems of the NPC converters is how to control the oscillation in the neutral point potential (NPP). If the NPP is not controlled effec-

tively, the output voltages of the converter wouldn't reach its reference values and the devices and equipment might be damaged. There are some modulation techniques that are able to completely eliminate the oscillations in NPP [5-7]. In [8] a dynamic limiter and a control loop are presented that provide the system with a fast balancing dynamic and guarantee stability under the all operating conditions. Also there are several nonlinear control methods [9-10] to maintain the output voltages balance. Reference [11] describes a new control method based on a simple feedback linearization procedure to obtain a linear time-invariant model for the NP voltage. The feedback linearization process takes almost no time, is direct, and yields a linear, time-invariant model. With this linear model, well-known and easy-to-implement classic control technique for obtaining the desired system response and disturbance rejection can be applied with greater accuracy than in previous approaches. [12] A nonlinear control strategy based on of feedback linearization technique is applied to the NPC converter. This control law robustness is validated for the various severe load and the system parameter variations. The input/output feedback linearization [13-15] control strategy that is proposed in this paper can enable the three phase/level NPC rectifiers to keep the output voltages and NPP at its desired values. Also, this control strategy is based on the dual lagrangian model [16] of the rectifier, which is obtained with the superposition law, the load current and the Euler-Lagrange description of the rectifier. Then, during the performance of the control strategy, the dynamics zero of the rectifier are avoided and the state feedback law controlled inputs are completed by pole placement.

The MATLAB/SIMULINK results comparing to the PI controller shown that the proposed control method gives good results in all the operating conditions such as: desired output voltages, very low THD, unity power factor and Neutral Point Potential (NPP) 0 V.

2 EULER-LAGRANGE MODELING OF THE 3 LEVEL/PHASE NPC RECTIFIER

The power circuit of the 3-level 3-phase NPC rectifier with balanced source is shown in Fig. 1. The output capacitors, line inductors and resistances are considered identical, i.e., $C_1 = C_2 = C$, $L_1 = L_2 = L_3 = L$ and $R_1 = R_2 = R_3 = R$ respectively. E_m is the amplitude of the input voltage source. S_{i1},S_{i2}, $\overline{S_{i1}}$ and $\overline{S_{i2}}$ (i=a, b, c) are switching functions describing the switching status of each phase as given by the following definition:

$$S_{ij} = \begin{cases} 0 & if\ T_{ij} = off \\ 1 & if\ T_{ij} = on \end{cases} \qquad i = a, b, c\ and\ \ j = 1, 2$$

Considering electric charges vector $q = [q_{La} \quad q_{Lb} \quad q_{Lc} \quad q_{C_1} \quad q_{C_2}]$ and currents vector

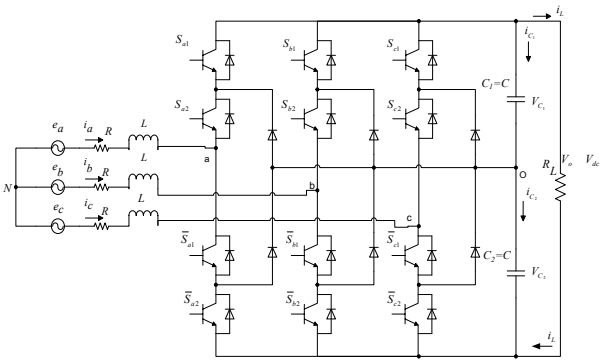

Fig. 1. Power circuit of three phase/level/leg voltage-sources NPC rectifier

$\dot{q} = [\dot{q}_{La} \quad \dot{q}_{Lb} \quad \dot{q}_{Lc} \quad \dot{q}_{C_1} \quad \dot{q}_{C_2}]$ corresponding to three boosting inductors and output capacitors respectively, the lagrangian of the system can be defined as:

$$\pounds(q, \dot{q}) = T(q, \dot{q}) - V(q), \tag{1}$$

where $T(q, \dot{q})$and $V(q)$ are magnetic co-energy and electric field energy of the circuit, respectively. In Fig. 1, the load current can be written both as:

$$i_L = (\dot{q}_{La} S_{a1} + \dot{q}_{Lb} S_{b1} + \dot{q}_{Lc} S_{c1}) - \dot{q}_{C_1}, \tag{2}$$

$$i_L = -(\dot{q}_{La} \overline{S_{a2}} + \dot{q}_{Lb} \overline{S_{b2}} + \dot{q}_{Lc} \overline{S_{c2}} + \dot{q}_{C_2}), \tag{3}$$

with $\overline{S_{ai}} = 1 - S_{ai}$. Of course, equation (2) is due to the capacitor C_1, and equation (3) is due to the capacitor C_2. Considering the load current presented above, the EL parameters describing the EL dynamics of the 3-level 3-phase NPC VSR can be written as:

$$T = \frac{1}{2} L \left(\dot{q}_{La}^2 + \dot{q}_{Lb}^2 + \dot{q}_{Lc}^2 \right), \tag{4}$$

$$V = \frac{1}{2C} q_{C_1}^2 + \frac{1}{2C} q_{C_2}^2, \tag{5}$$

$$D = \frac{1}{2} R \left(\dot{q}_{La}^2 + \dot{q}_{Lb}^2 + \dot{q}_{Lc}^2 \right) + \frac{1}{2} R_L \left\{ \dot{q}_{C_1} - (\dot{q}_{La} S_{a1} + \right.$$
$$\left. + \dot{q}_{Lb} S_{b1} + \dot{q}_{Lc} S_{c1}) \right\}^2, \tag{6}$$

or

$$D = \frac{1}{2} R \left(\dot{q}_{La}^2 + \dot{q}_{Lb}^2 + \dot{q}_{Lc}^2 \right) + \frac{1}{2} R_L \left\{ \dot{q}_{C_2} + (\dot{q}_{La} \overline{S_{a2}} + \right.$$
$$\left. + \dot{q}_{Lb} \overline{S_{b2}} + \dot{q}_{Lc} \overline{S_{c2}}) \right\}^2, \tag{7}$$

$$F = \begin{bmatrix} e_a & e_b & e_c & 0 & 0 \end{bmatrix}^T. \tag{8}$$

In these equations, the functions D and F are Rayleigh dissipation co-faction and the generalized forcing faction. Considering to the general from of the Euler–Lagrange (EL) equation:

$$\frac{d}{dt} \left(\frac{\partial \pounds}{\partial \dot{q}} \right) - \frac{\partial \pounds}{\partial q} + \frac{\partial D}{\partial \dot{q}} = F, \tag{9}$$

and by substituting the elements described above, the following equations can be achieved:

$$\frac{d}{dt}\left(\frac{\partial \mathrm{T}}{\partial \dot{q}_{La}}\right)-\frac{\partial \mathrm{T}}{\partial q_{La}}+\frac{\partial \mathrm{V}}{\partial q_{La}}+\frac{\partial D}{\partial \dot{q}_{La}}=e_a, \quad (10)$$

$$\frac{d}{dt}\left(\frac{\partial \mathrm{T}}{\partial \dot{q}_{Lb}}\right)-\frac{\partial \mathrm{T}}{\partial q_{Lb}}+\frac{\partial \mathrm{V}}{\partial q_{Lb}}+\frac{\partial D}{\partial \dot{q}_{Lb}}=e_b, \quad (11)$$

$$\frac{d}{dt}\left(\frac{\partial \mathrm{T}}{\partial \dot{q}_{Lc}}\right)-\frac{\partial \mathrm{T}}{\partial q_{Lc}}+\frac{\partial \mathrm{V}}{\partial q_{Lc}}+\frac{\partial D}{\partial \dot{q}_{Lc}}=e_c, \quad (12)$$

$$\frac{d}{dt}\left(\frac{\partial \mathrm{T}}{\partial \dot{q}_{C_1}}\right)-\frac{\partial \mathrm{T}}{\partial q_{C_1}}+\frac{\partial \mathrm{V}}{\partial q_{C_1}}+\frac{\partial D}{\partial \dot{q}_{C_1}}=0, \quad (13)$$

$$\frac{d}{dt}\left(\frac{\partial \mathrm{T}}{\partial \dot{q}_{C_2}}\right)-\frac{\partial \mathrm{T}}{\partial q_{C_2}}+\frac{\partial \mathrm{V}}{\partial q_{C_2}}+\frac{\partial D}{\partial \dot{q}_{C_2}}=0. \quad (14)$$

Since D is presented in equations (6) and (7), two direct calculation of (10)-(14) with the EL parameters are obtained.

The first calculation: considering the EL parameters (4)-(6), the following is obtained:

$$L\frac{d}{dt}(\dot{q}_{La})+R\dot{q}_{La}-R_L S_{a1}\big[\dot{q}_{C_1}-(\dot{q}_{La}S_{a1}+\dot{q}_{Lb}S_{b1}+\dot{q}_{Lc}S_{c1})\big]=e_a, \quad (15)$$

$$L\frac{d}{dt}(\dot{q}_{Lb})+R\dot{q}_{Lb}-R_L S_{b1}\big[\dot{q}_{C_1}-(\dot{q}_{La}S_{a1}+\dot{q}_{Lb}S_{b1}+\dot{q}_{Lc}S_{c1})\big]=e_b, \quad (16)$$

$$L\frac{d}{dt}(\dot{q}_{Lc})+R\dot{q}_{Lc}-R_L S_{c1}\big[\dot{q}_{C_1}-(\dot{q}_{La}S_{a1}+\dot{q}_{Lb}S_{b1}+\dot{q}_{Lc}S_{c1})\big]=e_c, \quad (17)$$

$$\frac{q_{C_1}}{C}+R_L\left[\dot{q}_{C_1}-(\dot{q}_{La}S_{a1}+\dot{q}_{Lb}S_{b1}+\dot{q}_{Lc}S_{c1})\right]=0, \quad (18)$$

$$\frac{q_{C_1}}{C}+R_L\left[\dot{q}_{C_2}+\left(\dot{q}_{La}\overline{S_{a2}}+\dot{q}_{Lb}\overline{S_{b2}}+\dot{q}_{Lc}\overline{S_{c2}}\right)\right]=0. \quad (19)$$

From (18), it follows:

$$\dot{q}_{C_1}-(\dot{q}_{La}S_{a1}+\dot{q}_{Lb}S_{b1}+\dot{q}_{Lc}S_{c1})=\frac{-q_{C_1}}{CR_L}. \quad (20)$$

By substituting (20) in equations (15)-(17), and by noting that $\dot{q}_{LK}=i_k$, $k=a,b,c$ and that voltage of the output capacitor C_1 can be written as: $V_{C_1}=q_{C_1}/C$, the EL model corresponding to the PWM converter can be described as:

$$L\frac{di_a}{dt}+Ri_a+S_{a1}V_{C_1}=e_a, \quad (21)$$

$$L\frac{di_b}{dt}+Ri_b+S_{b1}V_{C_1}=e_b, \quad (22)$$

$$L\frac{di_c}{dt}+Ri_c+S_{c1}V_{C_1}=e_c, \quad (23)$$

$$C\frac{dV_{C_1}}{dt}-(S_{a1}i_a+S_{b1}i_b+S_{c1}i_c)+\frac{V_{C_1}}{R_L}=0, \quad (24)$$

$$C\frac{dV_{C_2}}{dt}+(\overline{S_{a2}}i_a+\overline{S_{b2}}i_b+\overline{S_{c2}}i_c)+\frac{V_{C_2}}{R_L}=0. \quad (25)$$

Considering equations (21)-(25), it is possible to present them in the matrix form:

$$M\dot{\omega}+\xi_1(u)\,\omega+R\omega=F, \quad (26)$$

with

$$M=\begin{bmatrix} L & 0 & 0 & 0 & 0\\ 0 & L & 0 & 0 & 0\\ 0 & 0 & L & 0 & 0\\ 0 & 0 & 0 & C & 0\\ 0 & 0 & 0 & 0 & C \end{bmatrix},$$

$$\xi_1(u)=\begin{bmatrix} 0 & 0 & 0 & Sa1 & 0\\ 0 & 0 & 0 & Sb1 & 0\\ 0 & 0 & 0 & Sc1 & 0\\ -S_{a1} & -S_{b1} & -S_{c1} & 0 & 0\\ \overline{S_{a2}} & \overline{S_{b2}} & \overline{S_{c2}} & 0 & 0 \end{bmatrix},$$

$$R=\begin{bmatrix} R & 0 & 0 & 0 & 0\\ 0 & R & 0 & 0 & 0\\ 0 & 0 & R & 0 & 0\\ 0 & 0 & 0 & \frac{1}{R_L} & 0\\ 0 & 0 & 0 & 0 & \frac{1}{R_L} \end{bmatrix},$$

$$F=\begin{bmatrix} e_a & e_b & e_c & 0 & 0 \end{bmatrix}^T,$$

where $\omega=[i_a\ i_b\ i_c\ V_{C_1}\ V_{C_2}]$ and F is the vector consisting of voltage sources.

The second calculation: by considering the EL parameters (4), (5) and (7) similar to first calculation and by applying (10)-(14) to (4), (5) and (7), and by noting that $\dot{q}_{L_K}=i_k$, $k=a,b,c$ and that voltage of the output capacitor C_2 is $V_{C_2}=q_{C_2}/C$, and by considering that:

$$\dot{q}_{C_2}+(\dot{q}_{La}\overline{S_{a2}}+\dot{q}_{Lb}\overline{S_{b2}}+\dot{q}_{Lc}\overline{S_{c2}})=\frac{-q_{C_2}}{CR_L}, \quad (27)$$

the EL model corresponding to the converter can be written as:

$$L\frac{di_a}{dt}+Ri_a-\overline{S_{a_2}}V_{C_2}=e_a, \quad (28)$$

$$L\frac{di_b}{dt}+Ri_b-\overline{S_{b_2}}V_{C_2}=e_b, \quad (29)$$

$$L\frac{di_c}{dt}+Ri_c-\overline{S_{c_2}}V_{C_2}=e_c, \quad (30)$$

$$C\frac{dV_{C_1}}{dt}-(S_{a_1}i_a+S_{b_1}i_b+S_{c1}i_c)+\frac{V_{C_1}}{R_L}=0, \quad (31)$$

$$C\frac{dV_{C_2}}{dt}+(\overline{S_{a2}}i_a+\overline{S_{b2}}i_b+\overline{S_{c2}}i_c)+\frac{V_{C_2}}{R_L}=0. \quad (32)$$

The above equations will result in a matrix as follows:

$$M\dot{\omega} + \xi_2(u)\omega + R\omega = F, \tag{33}$$

with

$$\xi_2(u) = \begin{bmatrix} 0 & 0 & 0 & 0 & -\overline{S_{a2}} \\ 0 & 0 & 0 & 0 & -\overline{S_{b2}} \\ 0 & 0 & 0 & 0 & -\overline{S_{c2}} \\ -\overline{S_{a1}} & -\overline{S_{b1}} & -\overline{S_{c1}} & 0 & 0 \\ \overline{S_{a2}} & \overline{S_{b2}} & \overline{S_{c2}} & 0 & 0 \end{bmatrix},$$

where F, ω, M and R are identical for both calculations. M is a positive-definite diagonal matrix, R is the dissipation matrix and $\xi_i(u)$, $(i = 1, 2)$ is the interconnection matrix with switches. The energy balance equation is:

$$H(T) - H(0) + \int_0^T \omega^T R\omega dt = \int_0^T \omega^T F dt, \tag{34}$$

where $H = T + V = (1/2)\omega^T M$ represents the total energy of the circuit. Based on the energy balance equation:

$$\begin{aligned} &stored\ energy\ (H(T) - H(0))\ +\ dissipated \\ &energy \int_0^T \omega^T R\omega dt = \ supplied\ energy \int_0^T \omega^T F dt. \end{aligned}$$

Absentee of skew-symmetry property in the matrix F_i, $(i = 1, 2)$ has no effect on the energy balance equation. the derivative of energy balance equation (34) may be easily found by taking the derivative of H along the trajectory of (26) or (33).It is clear that the EL models (21)-(25) and (28)-(32) of 3-level 3-phase NPC rectifier are according to Kirchhoff's circuit theory and superposition law.

3 PROPOSED NONLINEAR CONTROL STRATEGY

3.1 Input/output feedback linearization based on the first equations (21- 25)

In this section, it is considered that the first equations to regulate output voltage V_{C_1} and PF (power factor), using input/output feedback linearization technique. By applying odq transformation [16] to (21-25), the first equations of the rectifier in a rotating reference frame d-q may be written as below:

$$L\dot{x}_1 = -Rx_1 + \omega L x_2 - S_{d1}x_3 + e_d, \tag{35}$$

$$L\dot{x}_2 = -Rx_2 - \omega L x_1 - S_{q1}x_3, \tag{36}$$

$$C\dot{x}_3 = \frac{3}{2}\left[(S_{d1}x_1 + S_{q1}x_2) - \frac{2}{3R_L}x_3\right], \tag{37}$$

$$C\dot{x}_4 = \frac{3}{2}\left[(S_{d2}x_1 + S_{q2}x_2) - \frac{2}{3R_L}x_4\right], \tag{38}$$

with: $\begin{bmatrix} x_1 & x_2 & x_3 & x_4 \end{bmatrix} = \begin{bmatrix} i_d & i_q & V_{C_1} & V_{C_2} \end{bmatrix}$.

On the other hand, according to (2), we will only consider the effect of capacitor C_1 to obtain the power balance between dc and ac sides, i.e.,

$$\frac{3}{2}e_d x_1 = x_3\left(i_L + C\frac{dx_3}{dt}\right). \tag{39}$$

For applying input/output feedback linearization to a nonlinear system, the number of control inputs u_i should be equal to the number of controlled outputs y_i. The control inputs of the system based on the first equations are:

$$u_{11} = S_{d1}, \qquad u_{21} = S_{q1}. \tag{40}$$

Thus, the system controlled outputs will be reduced as below:

$$y_{11} = x_2, \qquad y_{21} = x_3. \tag{41}$$

In order to obtain an effective linearized system, we should repeatedly differentiate each output y_{i1} $(i = 1, 2)$ until at least one input u_{i1} $(i = 1, 2)$ appears explicitly in its expression. After a straightforward calculation:

$$\dot{y}_{11} = \dot{x}_2 = \dot{i}_q = \frac{1}{L}\left(-Ri_q - \omega L i_d - S_{q1}V_{C_1}\right), \tag{42}$$

$$\begin{aligned} \ddot{y}_{21} = \ddot{x}_3 = \ddot{V}_{C_1} = &-\frac{3Re_d i_d}{2LCV_{C_1}} + \frac{3\omega e_d i_q}{2CV_{C_1}} - \frac{3e_d S_{d1}}{2LC} \\ &+ \frac{3e_d E_m}{2LCV_{C_1}} - \frac{9e_d^2 i_d^2}{4C^2V_{C_1}^3} + \frac{3e_d i_d i_L}{2C^2V_{C_1}^2} - \frac{\dot{i}_L}{C}. \end{aligned} \tag{43}$$

The new inputs v_{i1} $(i = 1, 2)$ based on the first equations will be obtained as:

$$v_{11} = \dot{y}_{11}, \quad v_{21} = \ddot{y}_{21}. \tag{44}$$

Relation (44) shows that there is a linear relation between the outputs and the new inputs. By Substituting (44) into (42) and (43) and also after some calculations, the switching functions of S_{d_1}, S_{q_1} are given as:

$$S_{q1} = \frac{1}{V_{C_1}}\left(-Ri_q - \omega L i_d - Lv_{11}\right), \tag{45}$$

$$\begin{aligned} S_{d1} = &-\frac{Ri_d}{V_{C_1}} + \frac{L\omega i_q}{V_{C_1}} + \frac{E_m}{V_{C_1}} - \frac{3Le_d i_d^2}{2CV_{C_1}^3} + \frac{Li_d i_L}{CV_{C_1}^2} \\ &- \frac{2L\dot{i}_L}{3e_d} - \frac{2LC}{3e_d}v_{21}. \end{aligned} \tag{46}$$

To guarantee unity power factor and regulate the voltage of C_1 capacitor, the new inputs are defined as:

$$\dot{i}_q = v_{11} = \dot{i}_q^* - \lambda_{11}\left(i_q - i_q^*\right), \qquad i_q^* = 0, \tag{47}$$

$$\begin{aligned} \ddot{V}_{C_1} = v_{21} = \ddot{V}_{C_1}^* - \gamma_{11}\left(\dot{V}_{C_1} - \dot{V}_{C_1}^*\right) - \\ - \gamma_{21}\left(V_{C_1} - V_{C_1}^*\right), \quad V_{C_1}^* = 250\ V, \end{aligned} \tag{48}$$

where i_q^* and $V_{C_1}^*$ are the reference value of i_q and V_{C_1}, respectively. The gains λ_{11} and γ_{i1}, $(i = 1, 2)$ can be designed by using linear techniques (poles assignment, LQR, etc.).

3.2 Input/output feedback linearization based on the second equations (28-32)

The second equations (28-32) in synchronous d-q frame are obtained as follows:

$$L\dot{x}_1 = -Rx_1 + \omega L x_2 - S_{d2}x_4 + E_m, \tag{49}$$

$$L\dot{x}_2 = -Rx_2 - \omega L x_1 - S_{q2}x_4, \tag{50}$$

$$C\dot{x}_3 = \frac{3}{2}\left[(S_{d1}x_1 + S_{q1}x_2) - \frac{2}{3R_L}x_3\right], \tag{51}$$

$$C\dot{x}_4 = \frac{3}{2}\left[(S_{d2}x_1 + S_{q2}x_2) - \frac{2}{3R_L}x_4\right], \tag{52}$$

with: $\left[\begin{array}{cccc} x_1 & x_2 & x_3 & x_4 \end{array}\right] = \left[\begin{array}{cccc} i_d & i_q & V_{C_1} & V_{C_2} \end{array}\right]$.

As it can be seen from equation (3), dc power is due to the effect of C_2 capacitor and the power balance between dc and ac sides will be as:

$$\frac{3}{2}e_d x_1 = x_4\left(i_L + C\frac{dx_4}{dt}\right). \tag{53}$$

The control inputs of the system based on the second equations are:

$$u_{12} = S_{d2} \quad u_{22} = S_{q2}. \tag{54}$$

It is known from (54) that the nonlinear control based on the second equations is completed by reducing the system outputs. Considering the reduced outputs, unity power factor and desired C_1 output voltage must be gained. Thus:

$$y_{12} = x_2 \quad y_{22} = x_4. \tag{55}$$

Applying input/output feedback linearization technique to (55):

$$\dot{y}_{12} = \dot{x}_2 = \dot{i}_q = \frac{1}{L}\left(-Ri_q - \omega L i_d - S_{q2}V_{C_2}\right), \tag{56}$$

$$\ddot{y}_{22} = \ddot{x}_4 = \ddot{V}_{C_2} = -\frac{3Re_d i_d}{2LCV_{C_2}} + \frac{3\omega e_d iq}{2CV_{C_2}} - \frac{3e_d S_{d2}}{2LC} + \frac{3e_d E_m}{2LCV_{C_2}} - \frac{9e_d^2 i_d^2}{4C^2V_{C_2}^3} + \frac{3e_d i_d i_L}{2C^2V_{C_2}^2} - \frac{\dot{i}_L}{C}. \tag{57}$$

The new inputs $v_{i2},\ (i = 1, 2)$ are:

$$v_{12} = \dot{y}_{12} \quad v_{22} = \ddot{y}_{22}. \tag{58}$$

By Substituting (58) into (56) and (57), the S_{d2} and S_{q2} are obtained as:

$$S_{q2} = \frac{1}{V_{C_2}}\left(-Ri_q - \omega L i_d - L v_{12}\right), \tag{59}$$

$$S_{d2} = -\frac{Ri_d}{V_{C_2}} + \frac{L\omega i_q}{V_{C_2}} + \frac{E_m}{V_{C_2}} - \frac{3Le_d i_d^2}{2CV_{C_2}^3} + \frac{Li_d i_L}{CV_{C_2}^2} - \frac{2L\dot{i}_L}{3e_d} - \frac{2LC}{3e_d}v_{22}. \tag{60}$$

The new inputs are considered as follows:

$$\dot{i}_q = v_{12} = \dot{i}_q^* - \lambda_{12}\left(i_q - i_q^*\right), \quad i_q^* = 0, \tag{61}$$

$$\ddot{V}_{C_2} = v_{22} = \ddot{V}_{C_2}^* - \gamma_{12}\left(\dot{V}_{C_2} - \dot{V}_{C_2}^*\right) - \gamma_{22}\left(V_{C_2} - V_{C_2}^*\right), \quad V_{C_2}^* = 250\ V, \tag{62}$$

where i_q^* and $V_{C_2}^*$ are the reference values of i_q and V_{C_2}, respectively.

3.3 The state feedback law

To control the new inputs, we use the state feedback controlled inputs as shown in (47), (48), (61) and (62). Then using a linear control technique, the gains $\lambda_{ij}\ \ (i = 1.j = 1, 2)$ and $\gamma_{ij}\ \ (i, j = 1, 2)$ will be obtained. First we define the output errors as below:

$$e_1 = i_q - i_q^*, \tag{63}$$

$$e_2 = V_{C_1} - V_{C_1}^*,\ e_3 = V_{C_2} - V_{C_2}^*. \tag{64}$$

By applying (63) and (64) to (47), (48), (61) and (62), two equation sets are obtained as:

$$\left\{\begin{array}{c} \dot{e}_1 + \lambda_{11}e_1 = 0 \\ \ddot{e}_2 + \gamma_{11}\dot{e}_2 + \gamma_{21}e_2 = 0 \end{array}\right. \quad \left\{\begin{array}{c} \dot{e}_1 + \lambda_{12}e_1 = 0 \\ \ddot{e}_3 + \gamma_{12}\dot{e}_3 + \gamma_{22}e_3 = 0 \end{array}\right. \tag{65}$$

By means of the pole placement technique the gains $\lambda_{ij}\ \ (i = 1,\ j = 1, 2)$ and $\gamma_{ij}\ \ (i,\ j = 1, 2)$ are obtained.

To control inner dynamics of system and eliminate the tracking error due to the presence of parasitic elements, we add integral controls to (65) and the new state feedback controlled inputs will be obtained as follows:

$$\left\{\begin{array}{c} \dot{e}_1 + \lambda_{11}e_1 + \lambda_{21}\int e_1 dt = 0 \\ \ddot{e}_2 + \gamma_{11}\dot{e}_2 + \gamma_{21}e_2 + \gamma_{31}\int e_2 dt = 0 \end{array}\right., \tag{66}$$

and

$$\left\{\begin{array}{c} \dot{e}_1 + \lambda_{12}e_1 + \lambda_{22}\int e_1 dt = 0 \\ \ddot{e}_3 + \gamma_{12}\dot{e}_3 + \gamma_{22}e_3 + \gamma_{32}\int e_3 dt = 0 \end{array}\right. . \tag{67}$$

The integral controls will cause robust control against parasitic elements. Now the pole placement technique is applied to (66) and (67) and then the gains $\lambda_{ij}\ \ (i, j = 1, 2)$ and $\gamma_{ij}\ \ (i = 1, 2,\ j = 1, 2, 3)$ are obtained.

3.4 Three-Level SPWM Modulation Method

We use 3-level SPWM for controlling the rectifier. Though the three-level SPWM modulation is nonlinear, it has the advantages of lower switching frequency and easier to be realized. The obtained switching functions from (45), (46), (59) and (60) are transformed into reference abc frame (switching functions S_{i1} and $S_{i2}\ \ (i = a, b, c)$) and then we define the switching signals $V_i\ \ (i = a, b, c)$ as below:

$$V_i = S_{i1}V_{C_1} + S_{i2}V_{C_2}, \quad i = a, b, c. \tag{68}$$

Modulation of phase "a" is denoted in Fig (2).

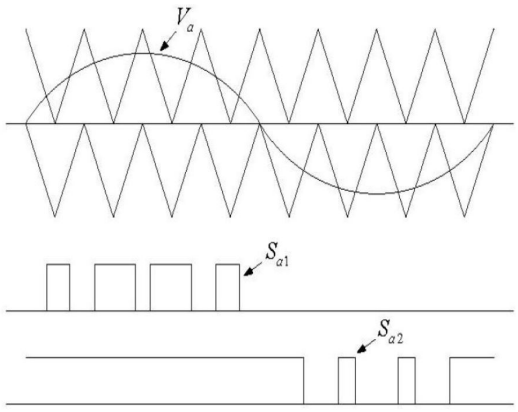

Fig. 2. Three-level SPWM

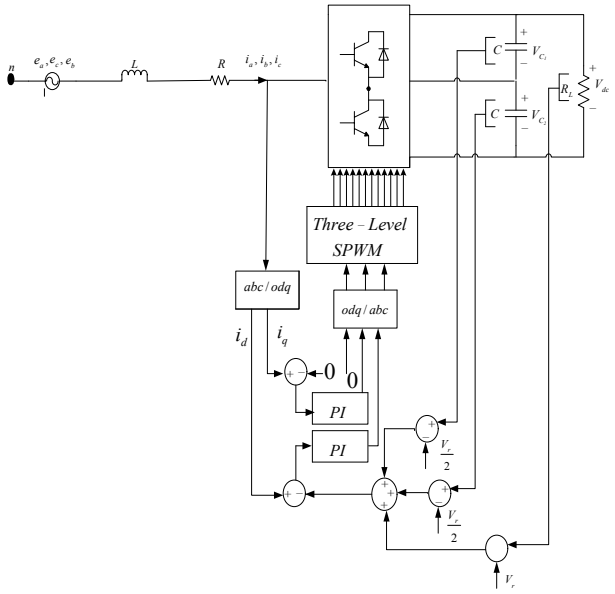

Fig. 3. Block diagram of the PI controller

4 PI CONTROLLER TECHNIQUE

A PI control technique for the NPC rectifier using MATLAB/SIMULINK is applied to compare with the proposed control method. In order to maintain the V_{C_1} and V_{C_2} output voltages and the neutral point potential at desired set point, the desired value of input d-component current is given as below:

$$x_1^* = \left(x_3 - \frac{V_r}{2}\right) + \left(x_4 - \frac{V_r}{2}\right) + (V_{dc} - V_r)\,. \quad (69)$$

Also, to guarantee unity power factor operation, the desired value of input q-component current is defined as:

$$x_2^* = 0. \quad (70)$$

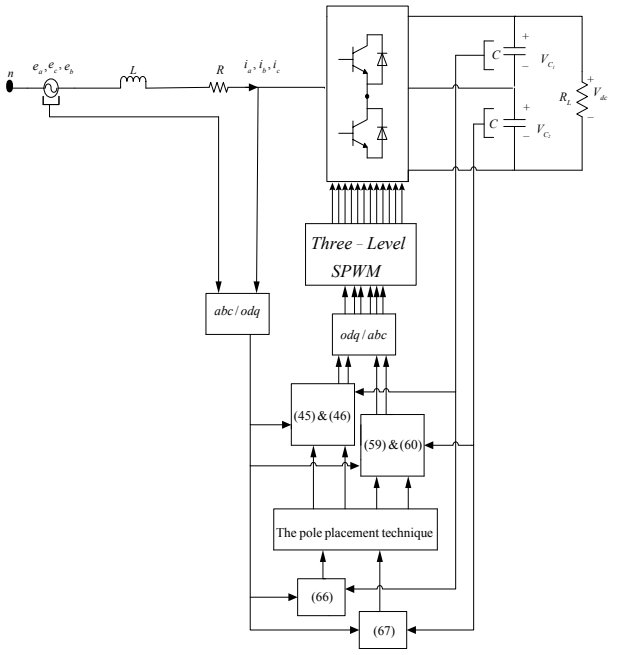

Fig. 4. Block diagram of the proposed control method

Using two desired values and PI controllers, the control method based on PI controller can be obtained as shown in Fig. 3.

5 SIMULATION RESULTS

To verify the proposed nonlinear control method, the three level/phase NPC rectifier has been studied by simulation using MATLAB/ SIMULINK and compared to the performance of the same system with a PI controller. Figure 4 shows the block diagram of the proposed nonlinear

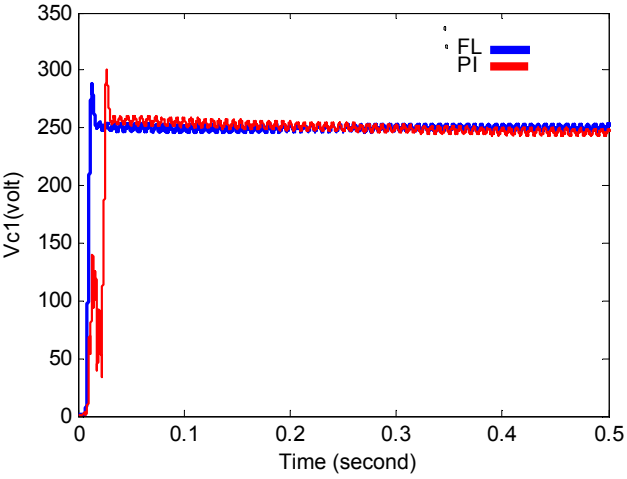

Fig. 5. The voltage of C_1 capacitor

control system. The parameters of the system are considered as: $R = 0.1\Omega$, $L = 0.003mH$, $R_L = 30\Omega$, $C = C_1 = C_2 = 2200\mu F$, $f = 50Hz$, switching frequency$= 2KHz$, $E_m = 150V$, $V_{dc} = V_r = 500V$, $V_{C_1} = V_{C_2} = 250V$.

As it can be seen from figures 5-7, the proposed nonlinear controller can keep the output voltages near their desired values and also the Neutral Point Potential (NPP) approaches to zero (the voltage $V_{C_1} - V_{C_2}$ of is near zero).

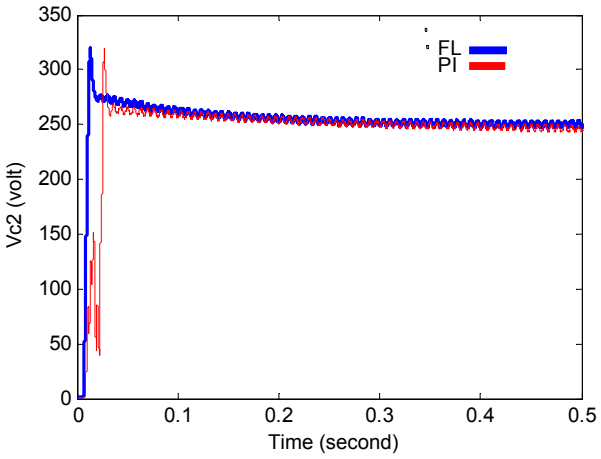

Fig. 6. The voltage of C_2 capacitor

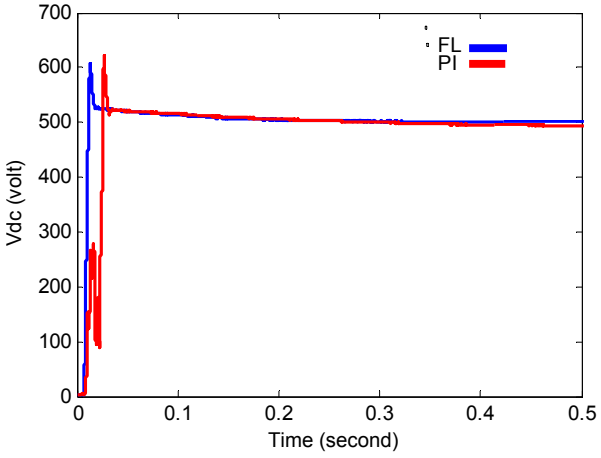

Fig. 7. Dc-link output voltage

The results show that the transient state of FL is shorter than PI controller and maintains better output voltages at desired values in steady state. Figures 8-9 show that the system can reach unity power factor and the line-current is nearly a sine wave. In comparison, the proposed control method is superior to PI controller. Figure 10 shows the values of the line-current THD in the steady state. However, PI controller has a slight superiority, the obtained

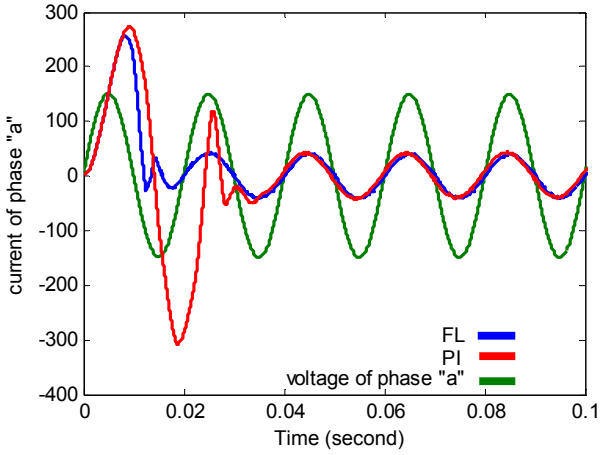

Fig. 8. Current and voltage of phase a

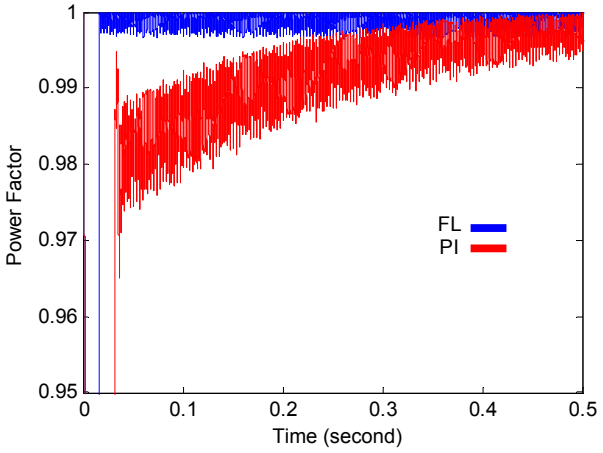

Fig. 9. Power factor

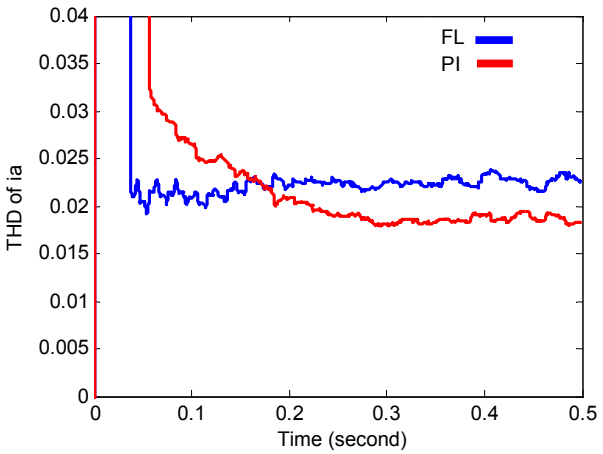

Fig. 10. THD of the i_a

THD value is 2.3% for FL and therefore meets the standards IEC 61 000-3-2/4.

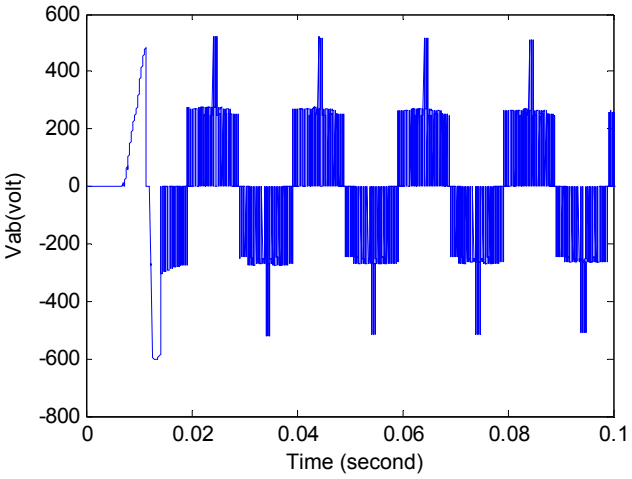

Fig. 11. The input line-line voltage V_{ab} for FL

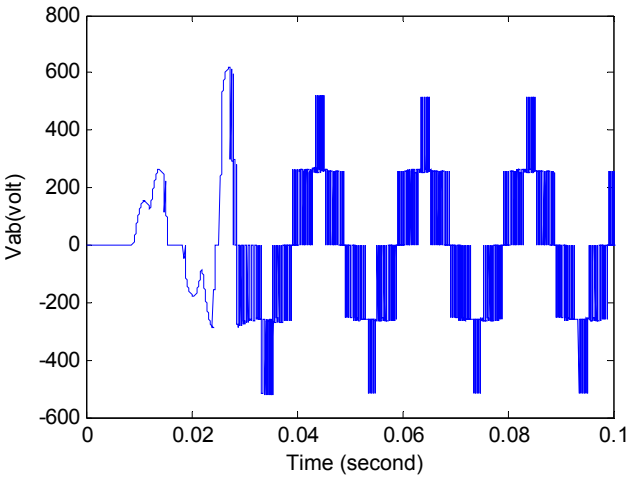

Fig. 12. The input line-line voltage V_{ab} for PI

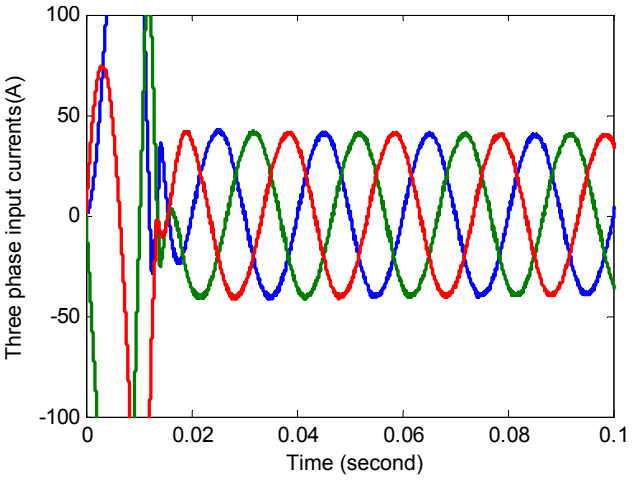

Fig. 13. Three-phase input current for FL

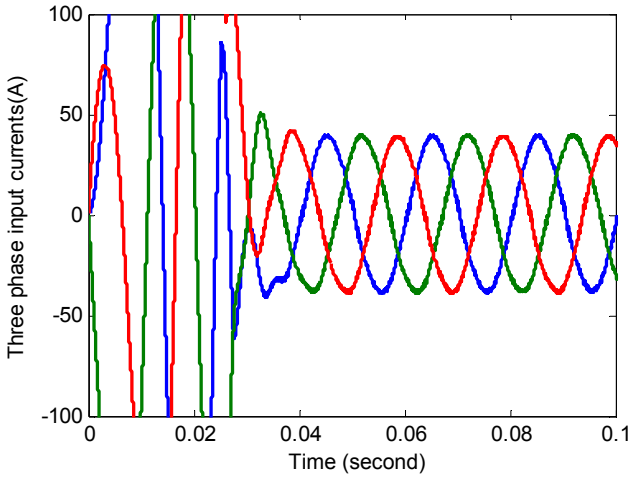

Fig. 14. Three-phase input current for PI

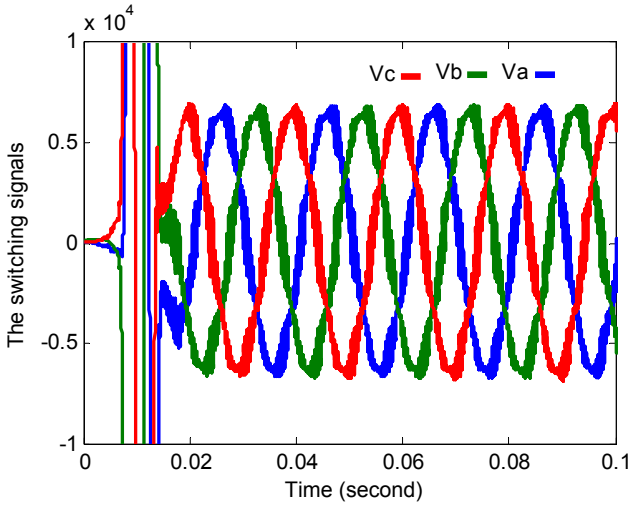

Fig. 15. The switching signals for FL

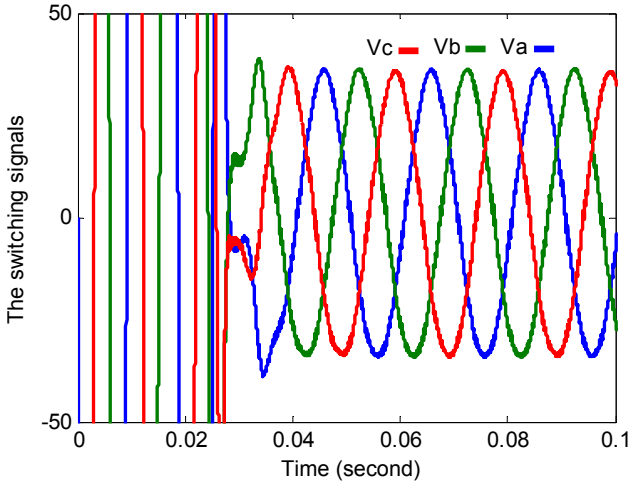

Fig. 16. The switching signals for PI

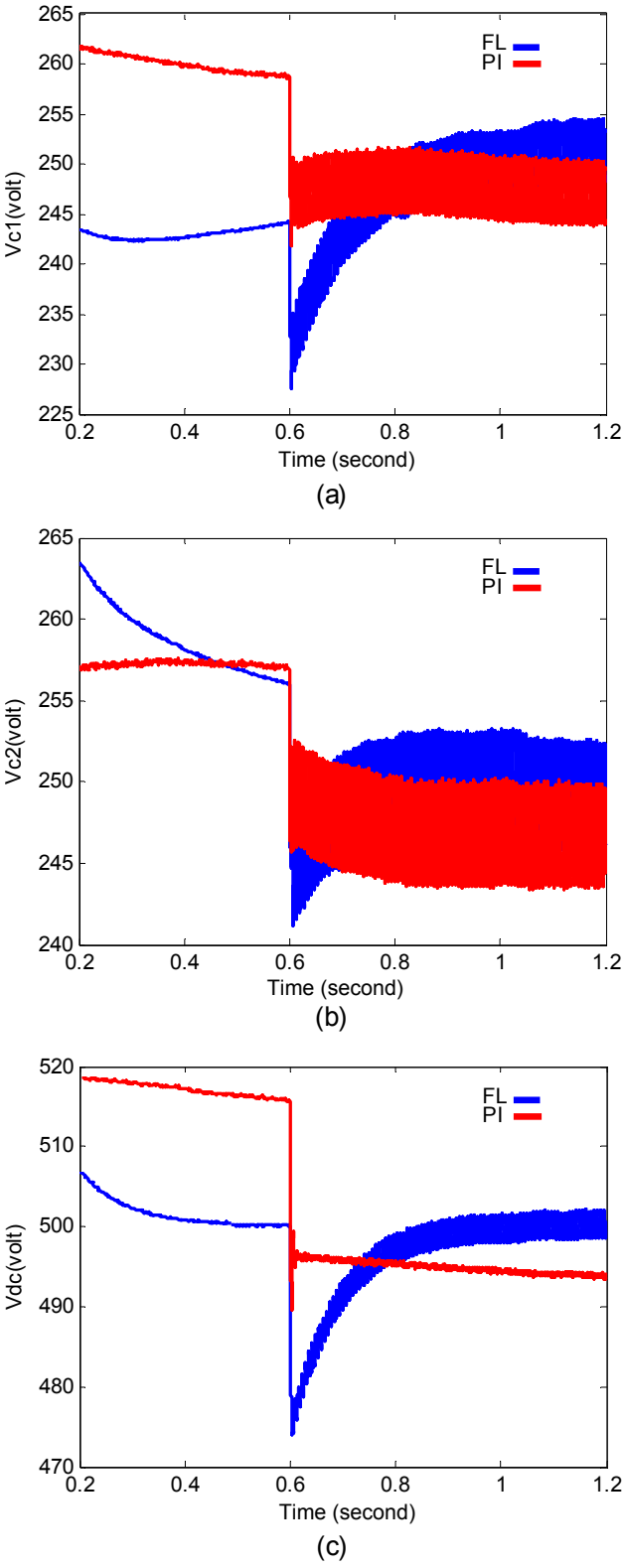

Fig. 17. (a-c): Response of output voltages with a step changes in the load current from zero to nominal value in $t = 0.6\ s$

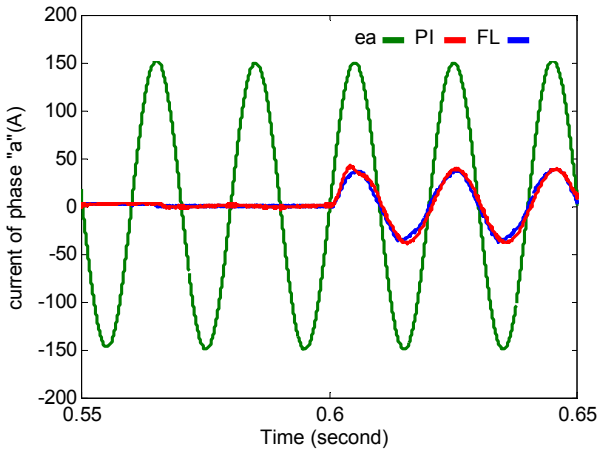

Fig. 18. Response of current and voltage of phase a with a step changes in the load current from zero to nominal value in $t = 0.6\ s$

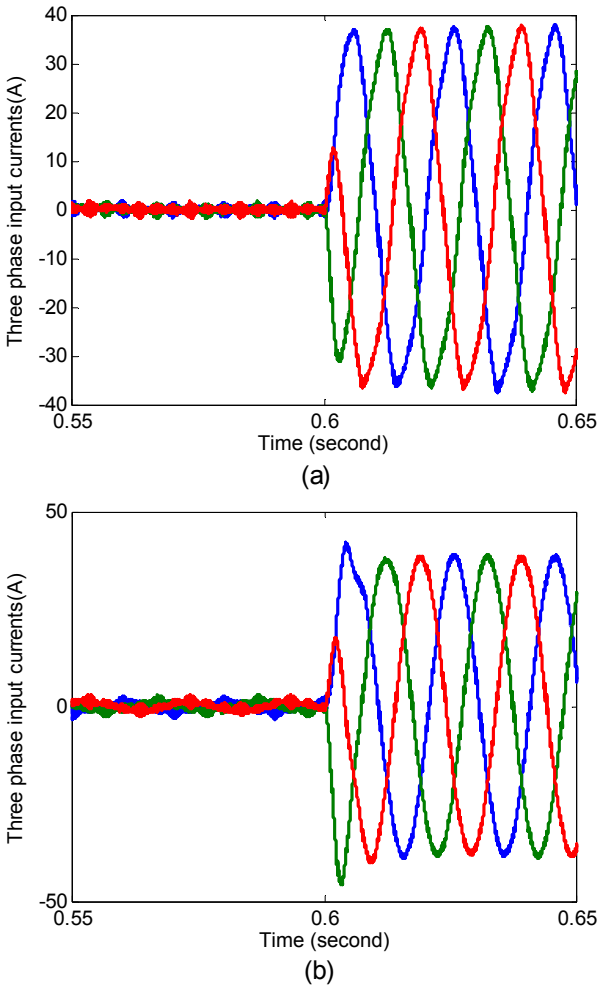

Fig. 19. Response of three phase input currents with a step changes in the load current from zero to nominal value in $t = 0.6\ s$ (a) FL, (b) PI

The input line-to-line voltage (V_{ab}) of the rectifier is shown in figures 11-12. Figures 13-14 show three phase input currents in steady state operation for FL and PI controller, respectively. The switching signals of the two controllers are shown in Figs 15 and 16. In all of the mentioned figures, FL controller has an extremely short transient state and can reach their desired values quickly.

The response of the output voltages for a step change in the load current from zero to nominal value at $t = 0.6$ s is shown in Fig. 17 (a-c). The proposed controller reduces the steady-state error and indicates faster performance and less undershoot compared to the PI controller. Fig. 18 shows the response of current and voltage of phase "a" with a step changes in the load current from zero to nominal value at $t = 0.6$ s. It clearly shows that FL controller performs well by allowing input current to be tracked at the desired value with maintaining unit PF. Figs. 19(a-b) and 20(a-b) show the response of three phase input currents and switching signals with step changes in the load current from zero to nominal value at $t = 0.6$ s validate the proposed nonlinear control robustness against the sudden change of load.

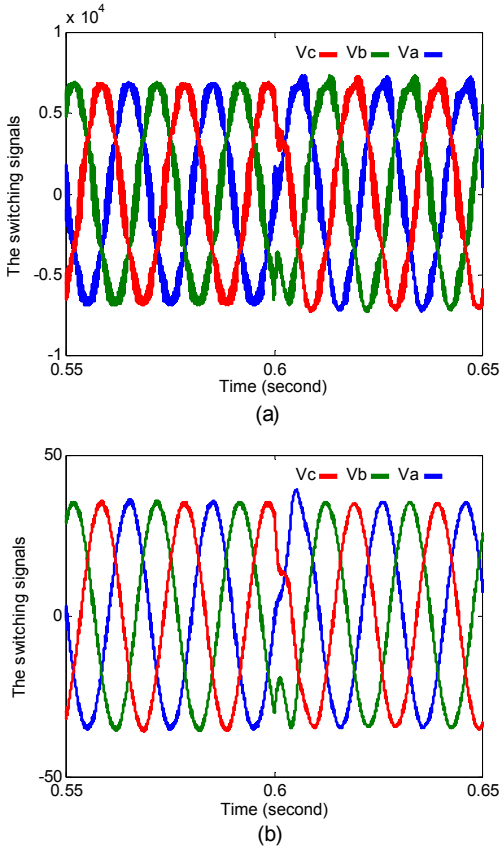

Fig. 20. Response of the switching signals with a step changes in the load current from zero to nominal value in $t = 0.6$ s (a)FL, (b) PI

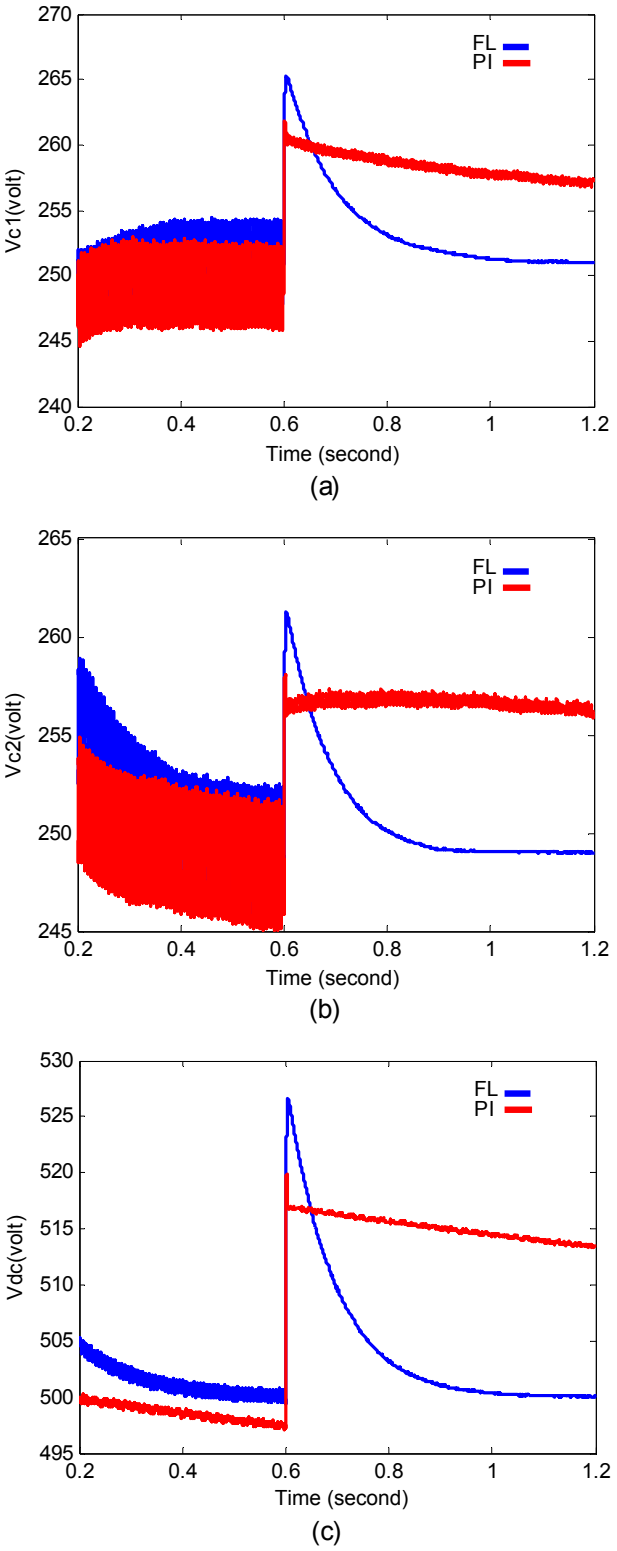

Fig. 21. (a-c). Response of dc-link output voltage with a step changes in the load current from nominal value to zero in $t = 0.6$ s

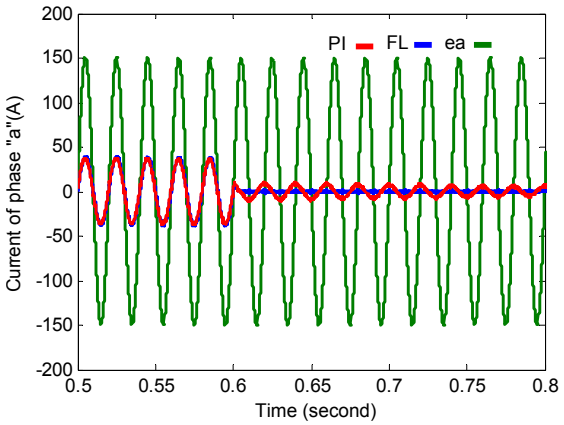

Fig. 22. Response of current and voltage of phase a with a step changes in the load current from nominal value to zero in $t = 0.6$ s

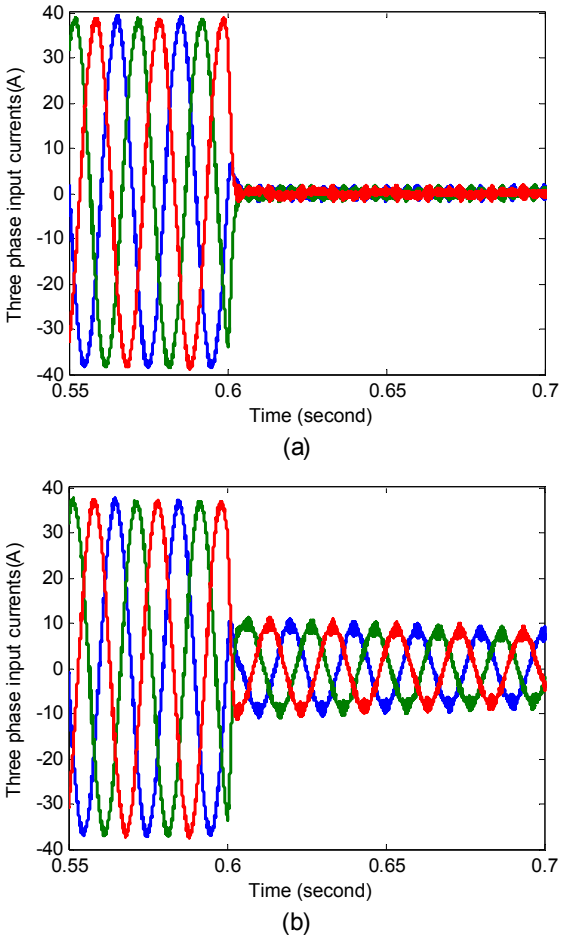

Fig. 23. Response of three phase input currents with a step changes in the load current from nominal value to zero in $t = 0.6$ s (a) FL, (b) PI

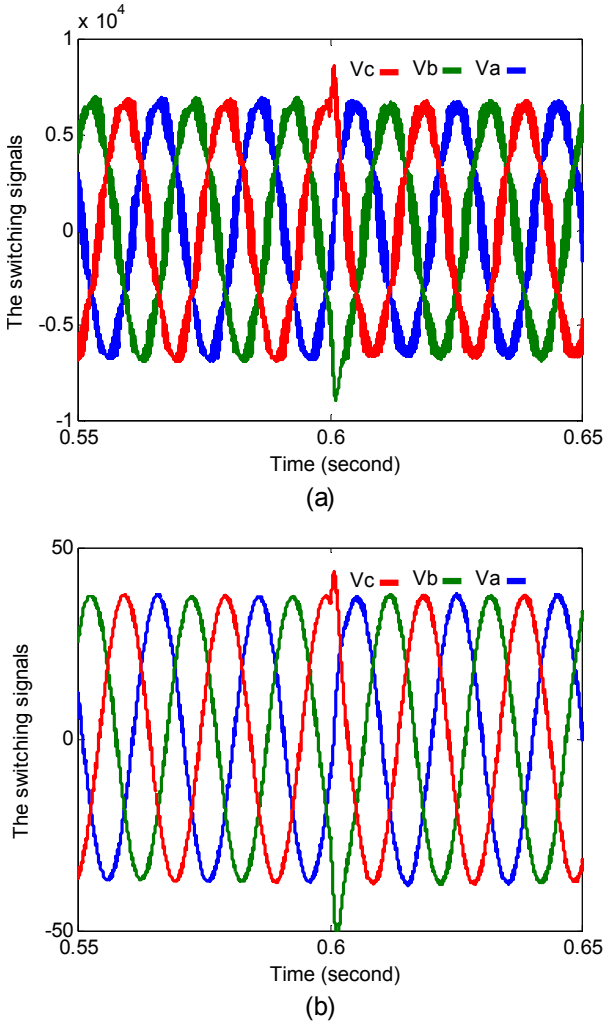

Fig. 24. Response of the switching signals with a step changes in the load current from nominal value to zero in $t = 0:6$ s (a) FL, (b) PI

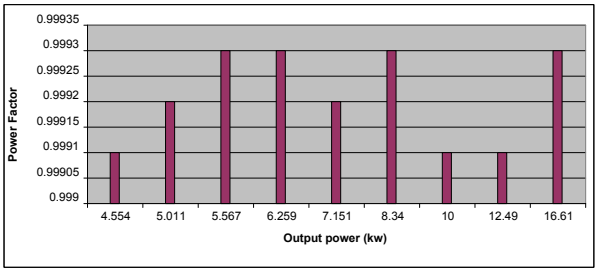

Fig. 25. Power Factor under different output power

Figure 21 (a-c) shows the response of dc-link output voltages with a step Changes in the load current from nominal value to zero in $t = 0.6$ s. Due to a change in system load, the output voltages are disturbed and are again sta-

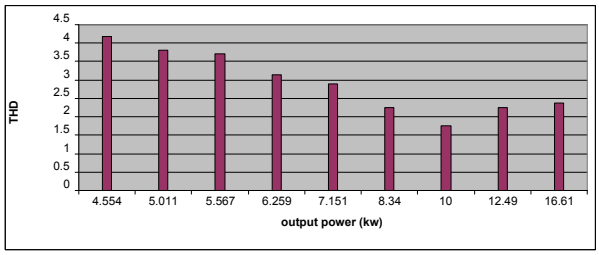

Fig. 26. THD under different output power

bilized faster by using the proposed nonlinear controller in comparison to the PI controller. The output voltage overshoots are extremely small and the proposed nonlinear controller can keep the output voltages at their desired value. Also the response of current and voltage of phase "a" with a step changes in the load current from nominal value to zero in $t = 0.6$ s is shown in Fig. 22. Figure 22 shows the performance superiority of the proposed controller in reaching the current of phase "a" to zero during the load variation. It can be understood from Fig. 23 (a-b) and Fig. 24 (a-b) that the three phase input currents and the switching signals variations are extremely small and also in comparison with PI controller, the proposed nonlinear control law has better input currents and switching signals in keeping at their desired value. Figures 25 and 26 show the power factor and THD of phase "a" current, under the different load conditions for FL.

6 CONCLUSION

In this paper, a nonlinear controller based on input/output feedback linearization technique and a new model of the three level/phase NPC rectifier has been proposed. After obtaining dual lagrangian model of the rectifier using the Euler-Lagrange description of the rectifier, the superposition law and the two obtained forms of the load current, two the power-balance equations between the ac and dc sides are obtained by considering its corresponding load current. Then, the system is linearized and also the state feedback law controlled inputs are designed. To achieve a robust control against parasitic elements, some integrators are added to the state feedback law and then the new controlled inputs are completed by pole placement technique. Defining the appropriate outputs, the presented linearizing control law can avoid the zero dynamics of the system. The proposed control technique is also validated for dc-bus voltages tracking, unity power factor and very low THD reaching by MATLAB/SIMULINK. In comparison with PI controller, the proposed controller has a significant superiority.

REFERENCES

[1] J. Li, S. Bhattacharya, and A. Q. Huang,, "A New Nine-Level Active NPC (ANPC) Converter for Grid Connection of Large Wind Turbines for Distributed Generation," *IEEE Trans on Power Electronics, Vol. 26, No. 3, March 2011, pp. 961–972.*

[2] M. Chaves, E. Margato, J.F. Silva, S.F. Pinto, J. Santana,, "Fast optimum-predictive control and capacitor voltage balancing strategy for bipolar back-to-back NPC converters in high-voltage direct current transmission systems," *IET Gener. Transm. Distrib., 2011, Vol. 5, Iss. 3, pp. 368–375.*

[3] H. Akagi, K. Isozaki, "A Hybrid Active Filter for a Three-Phase 12-Pulse Diode Rectifier Used as the Front End of a Medium-Voltage Motor Drive," *IEEE Trans on Power Electronics, Vol. 27, NO. 1. January 2012 pp. 69–77.*

[4] G. Abad, M. Á. Rodríguez, J. Poza, " Three-Level NPC Converter-Based Predictive Direct Power Control of the Doubly Fed Induction Machine at Low Constant Switching Frequency," *IEEE Transactions on Industrial Electronics, VOL. 55, NO. 12, DECEMBER 2008, pp. 4417-4429.*

[5] J. Pou, J. Zaragoza, P. Rodríguez, S. Ceballos, V. Sala, R. Burgos, and D. Boroyevich, "Fast-processing modulation strategy for the neutral-point-clamped converter with total elimination of the low-frequency voltage oscillations in the neutral point," *IEEE Trans. Ind. Electron., vol. 54, no. 4, pp. 2288–2299, Aug. 2007.*

[6] S. Busquets-Monge, J. D. Ortega, J. Bordonau, J. A. Beristáin, and J. Rocabert, "Closed-loop control design for a three-level three-phase neutral-point-clamped inverter using the optimized nearest-three virtual space-vector modulation," *in Proc. IEEE PESC, 2006, pp. 1–7.*

[7] S. Busquets-Monge, J. Bordonau, D. Boroyevich, and S. Somavilla,"The nearest three virtual space vector PWM—A modulation for the comprehensive neutral-point balancing in the three-level NPC inverter," IEEE Power Electron. Lett., vol. 2, no. 1, pp. 11–15, Mar. 2004.

[8] J. Zaragoza, J. Pou, S. Ceballos, E. Robles, C. Jaen, and M. Corbalán "Voltage -Balance Compensator for a Carrier-Based Modulation in the Neutral-Point-Clamped Converter," *IEEE Trans on Industrial Elec*, vol. 56, no. 2. pp, 305–314, Feb 2009.

[9] A. Isidori, Nonlinear Control Systems, 2nd ed. Berlin, Germany: Springer-Verlag, 1995.

[10] J. E. Slotine andW. Li, Applied Nonlinear Control. Englewood Cliffs, NJ: Prentice–Hall, 1991.

[11] S. Cobreces, J. Bordonau, J. Salaet, E. J. Bueno, F. J. Rodriguez, "Exact Linearization Nonlinear Neutral-Point Voltage Control for Single-Phase Three-Level NPC Converters," *IEEE Trans on Power Elec*, vol. 24, no. 10,. pp, 2357–2362, Oct. 2009.

[12] L..Yacoubi,K..Al-Haddad, F..Fnaiech and L..A.Dessaint, "A DSP-Based Implementation of a New Nonlinear Control for a Three-Phase Neutral Point Clamped Boost Rectifier Prototype," *IEEE Transactions on Industrial Electronics* vol. 52. No.1. Feb. 2005, pp. 197-205.

[13] T.-S. Lee, "Input-output linearization and zero-dynamics control of three-phase ac/dc voltage-source converters," *IEEE Transactions on Power Electronics*, vol. 18, pp. 11–22, Jan. 2003.

[14] D.-C. Lee, G.-M. Lee, and K.-D. Lee, "Dc-bus voltage control of three-phase ac/dc pwm converters using feedback linearization," *IEEE Transactions on Industry Applications*, vol. 36, pp. 826–833, May-June 2000.

[15] A. E. Leon, J. A. Solsona, C. Busada, H. Chiacchiarini, M. I. Valla "A Novel Feedback/Feed forward Control Strategy for Three-Phase Voltage-Source Converters," *1-4244-0755-9/07 '2007 IEEE, pp. 3391–3396.*

[16] M. Mehrasa , S. Lesan , S. N. Hoseini Emeni, A. Sheikholeslami ,"Passivity-Based Control With Dual Lagrangian Model Of Four-Wire Three-Level Three-Phase NPC Voltage-Source Rectifier ", *Special Power Electronics Systems and Applications, CPE, IEEE*, pp.411-418., 2009.

Majid Mehrasa was born in Iran, on September 1983. He received the B.S. and M.S. degrees in Electrical Engineering from Noshirvani University, Babol, Iran, in 2006 and 2009, respectively. His research interests are nonlinear control and observation with applications to control of electric power converters and application of power electronics to power systems.

Masoud Ahmadigorji was born in Sari, Iran, on August 1984. Obtained his B.Sc and M.Sc. Degrees in Electrical Engineering from Khajeh-Nasir Toosi University of Technology and Sharif University of Technology, Tehran, Iran in 2006 and 2008, respectively. Currently, he is Ph.D. student in Power Electrical Engineering at Semnan University, Semnan, Iran. His areas of interest are power system optimization, Distribution system planning, Distributed Generation (DG), and application of power electronic in power system.

Nima Amjady was born in 1971 in Tehran, Iran. He received the B.Sc., M.Sc., and Ph.D. degrees in electrical engineering from Sharif University of technology, Tehran, in 1992, 1994 and 1997, respectively. At present, he is professor with the Electrical Engineering Department, Semnan University, Semnan, Iran. His research interests include security assessment of power systems, reliability of power networks, load and price forecasting, artificial intelligence and its application to the problems of power systems.

AUTHORS' ADDRESSES

Majid Mehrasa, M.Sc.
Department of Power Engineering,
Faculty of Electrical and Computer Engineering,
Noshirvani Babol University of Technology,
Shariati Av. 484, IR-47148-71167, Babol, Mazandaran, Iran
email: m.majidmehrasa@gmail.com

Masoud Ahmadigorji, M.Sc.
Prof. Nima Amjady, Ph.D.
Department of Power Engineering,
Faculty of Electrical and Computer Engineering,
Semnan University,
Mowlawi Boulevard, Motahari Square, IR-35196-45399,
Semnan, Iran
email: m.ahmadigorji@alum.sharif.edu,
n_amjady@yahoo.com

Received: 2012-04-01
Accepted: 2012-12-21